Hijacked senescence secretomes as 'immune primers' of antiangiogenic TKI efficacy

Melissa Dolan, Yuhao Shi, James Hill, Michalis Mastri, Cristina Vaghi, Joseph Barbi, Sébastien Benzekry, John Ebos

▶ **To cite this version:**

Melissa Dolan, Yuhao Shi, James Hill, Michalis Mastri, Cristina Vaghi, et al.. Hijacked senescence secretomes as 'immune primers' of antiangiogenic TKI efficacy. AACR 2021, Apr 2021, Virtual meeting, United States. 81 (13_Supplement), pp.3195-3195, 2021, ⟨10.1158/1538-7445.AM2021-3195⟩. ⟨hal-04571502⟩

HAL Id: hal-04571502

https://inria.hal.science/hal-04571502v1

Submitted on 14 May 2024

HAL is a multi-disciplinary open access archive for the deposit and dissemination of scientific research documents, whether they are published or not. The documents may come from teaching and research institutions in France or abroad, or from public or private research centers.

L'archive ouverte pluridisciplinaire **HAL**, est destinée au dépôt et à la diffusion de documents scientifiques de niveau recherche, publiés ou non, émanant des établissements d'enseignement et de recherche français ou étrangers, des laboratoires publics ou privés.

Distributed under a Creative Commons CC BY 4.0 - Attribution - International License

Investigating hijacked senescence secretomes as ‘immune primers’ following antiangiogenic TKI resistance

Melissa Dolan[1], Yuhao Shi[1], James W. Hill[5], Michalis Mastri[2], Cristina Vaghi[6,7], Joseph Barbi,[3] Sebastien Benzekry[6,7], John M.L. Ebos[1,2,4]

[1]Department of Experimental Therapeutics, [2]Department of Cancer Genetics, [2]Department of Cancer Genetics,[3] Department of Immunology, [4]Department of Medicine, Roswell Park Comprehensive Cancer Center; [5]Jacobs School of Medicine and Biomedical Sciences, SUNY at Buffalo; [6]Inria Team MONC, Inria Bordeaux Sud-Ouest, [7]Institut de Mathematiques de Bordeaux, CNSR UMR 5251, Bordeaux University, Talence, France.

ROSWELL PARK COMPREHENSIVE CANCER CENTER

DO NOT POST

Follow Us:
@mdolan1118
@EbosLab

Abstract

VEGF receptor tyrosine kinase inhibitors (VEGFR TKIs) and immune checkpoint inhibitors (ICIs) are approved together as a treatment regimen for multiple metastatic cancers, yet the mechanistic basis for this combinatory benefit remains unclear. Previously we have shown that resistance to VEGFR TKI treatment can transiently hijack the secretory machinery typically associated with senescence - the process of cellular aging. Here we report that these senescence-associated secretory programs can also drive immune cell activation, potentially ‘priming’ the tumor for PD-1 pathway inhibition. Using a novel live-cell sorting method based on C_{12}FDG – a substrate for senescence-associated beta-galactosidase activity – we isolated senescence-marker (SM) expressing VEGFR TKI-treated cells for transcriptomic analysis. SM+ cell populations were enriched for senescence, immune, and interferon secretory processes, with a unique gene signature validated using published preclinical and clinical datasets. Notably, SM+ cells were found to be more sensitive to CD8 T-cell mediated tumor inhibition *in vivo* and *ex vivo* and be sensitive to PD-L1 blockade. Together, these results suggest VEGFR TKI controlled secretory programs contributing to resistance can simultaneously prime the tumor microenvironment for immune cell activation, providing an explanation for improved effects of antiangiogenic and immunotherapy combinations or treatment sequences in patients.

① Isolation of live Senescence-marker (SM) cells following antiangiogenic TKI resistance

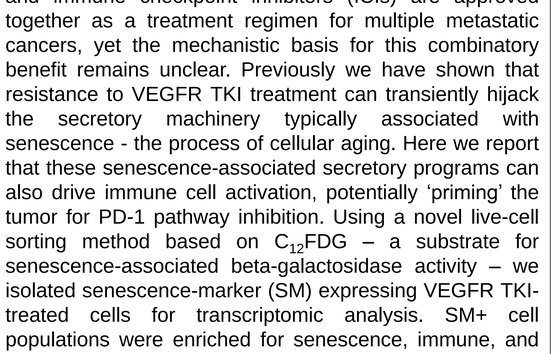

Figure 1: Selecting live Senescence-marker (SM) expressing tumor cells from antiangiogenic TKI resistant *in vivo* derived tumor cells. (A) Schematic showing *in vivo* derivation of antiangiogenic TKI resistant murine breast tumor cells selected from metastatic lesions following surgical resection of an orthotopically implanted tumor during VEGFR TKI treatment (i.e. Axitinib or Cabozantinib)[1]. **(B)** Quantification of senescence-marker (via SAβgal activity) expressing cells in 4T1 P and AxR cells (n = 5; left) and EMT6 P and CaR cells (n = 9; right) following incubation with C_{12}FDG (fluorescent β-gal substrate; 33μM; 60-80 min) after treatment with Bafilomycin A1 (lysosomal V-ATPase inhibitor; 100nM; 60 min)[1]. **(C)** Representative FACS schematic of C_{12}FDG-incubated 4T1 AxR cells that are sorted into live $SM^+/C_{12}FDG^+$ and $SM^-/C_{12}FDG^-$ cell populations.** *p<0.01; **** *p<0.0001; determined by t-test.*

1) Mastri, M., et al. (2018). A Transient Pseudosenescent Secretome Promotes Tumor Growth after Antiangiogenic Therapy Withdrawal. Cell Reports 25(13):3706-3720.e8

② Senescence and immune pathways are enriched in SM+ cells after antiangiogenic TKI resistance

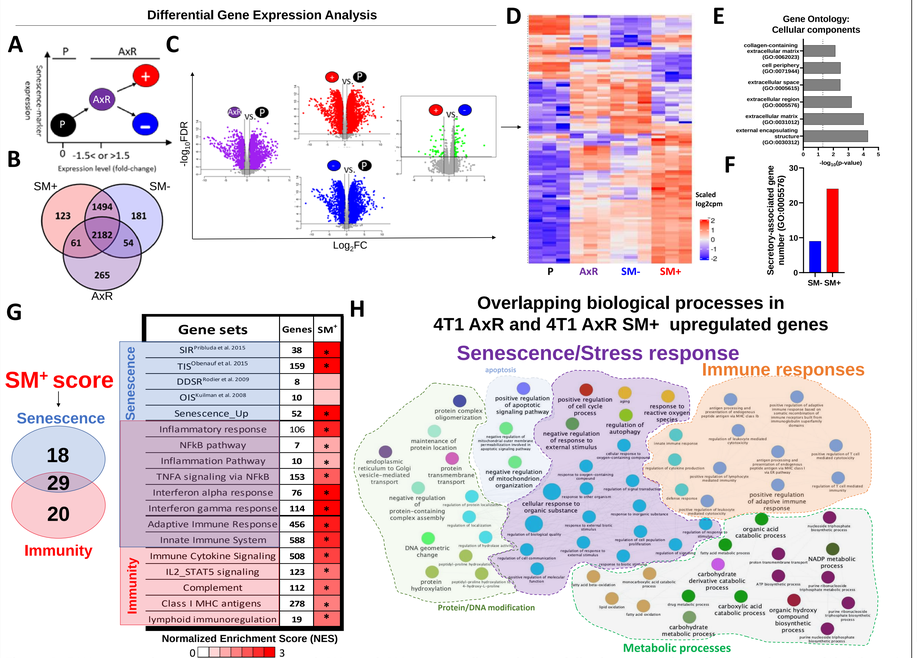

Figure 2: RNA-sequencing analysis of live sorted SM+ and SM- tumor cell populations following antiangiogenic TKI resistance. (A) Schematic mapping gene expression changes in sorted 4T1 AxR SM+ (red) and 4T1 AxR SM- (blue) cells. **(B)** Venn diagram representing shared and unique differentially expressed genes (DEGs) (all groups compared to 4T1 P; (Log_2 [Fold Change] ≤ -1.5 or ≥ 1.5; FDR ≤ 0.05). **(C)** Volcano plots showing DEGs in 4T1 cell variants with the following comparisons of interest: 4T1 AxR compared to 4T1 P (left; purple), 4T1 AxR SM- compared to 4T1 P (middle bottom; blue), 4T1 AxR SM^+ compared to 4T1 P (middle top; red), and 4T1 AxR SM+ compared to 4T1 AxR SM- (right; green) (SM+ and SM-: n = 3; biological replicates). (**D**) Heatmap showing gene expression changes unique to 4T1 AxR SM+ cells in 4T1 cell variants. (**E**) Gene Ontology (GO) analysis of uniquely upregulated genes in 4T1 AxR SM+ for significantly enriched cellular component terms. (**F**) Bar graph of uniquely upregulated secretory genes (identified by GO term: GO:0005576) in 4T1 AxR SM+ and 4T1 AxR SM-. (**G**) Number of genes within SM+ score associated with senescence, immunity, or both (right) and 4T1 AxR SM+ were assessed for enrichment of gene sets involved in published secretomes induced by therapy or senescence (blue) and gene sets from canonical/hallmark pathways involved in immunity (red) or involved in both (purple) by Gene Set Enrichment Analysis (GSEA) (C2, Molecular Signatures Database Collection; left). (**H**) GO analysis visualized with ClueGO in cytoscape of overlapping biological process terms in upregulated genes in 4T1 AxR and 4T1 AxR SM+ cells (grouped by terms related to biological processes). Sizes of circles correspond to FDR significance of each process and lines/edges represent term-term interactions defined by Kappa score. ** FDR < 0.05 indicating significance in GSEA.*

③ SM+ score is increased in TKI-treated patients

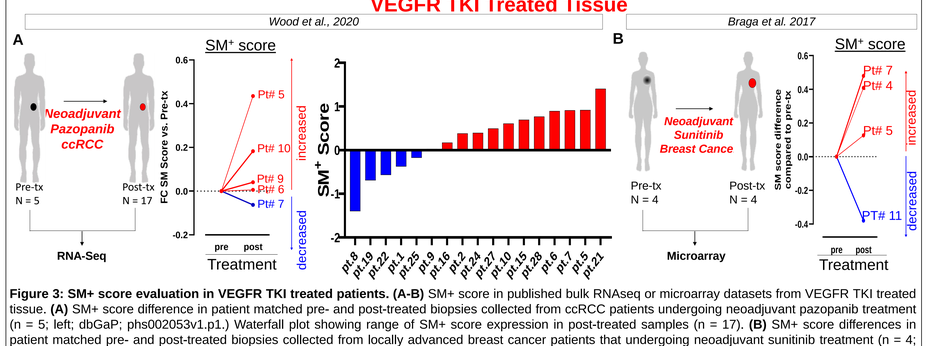

Figure 3: SM+ score evaluation in VEGFR TKI treated patients. (A-B) SM+ score in published bulk RNAseq or microarray datasets from VEGFR TKI treated tissue. **(A)** SM+ score difference in patient matched pre- and post-treated biopsies collected from ccRCC patients undergoing neoadjuvant pazopanib treatment (n = 5; left; dbGaP; phs002053v1.p1.) Waterfall plot showing range of SM+ score expression in post-treated samples (n = 7). **(B)** SM+ score differences in patient matched pre- and post-treated biopsies collected from locally advanced breast cancer patients that undergoing neoadjuvant sunitinib treatment (n = 4; GEO:GSE58837).

④ SM+ cells are enriched for IFN regulated genes including MHC I and PDL1

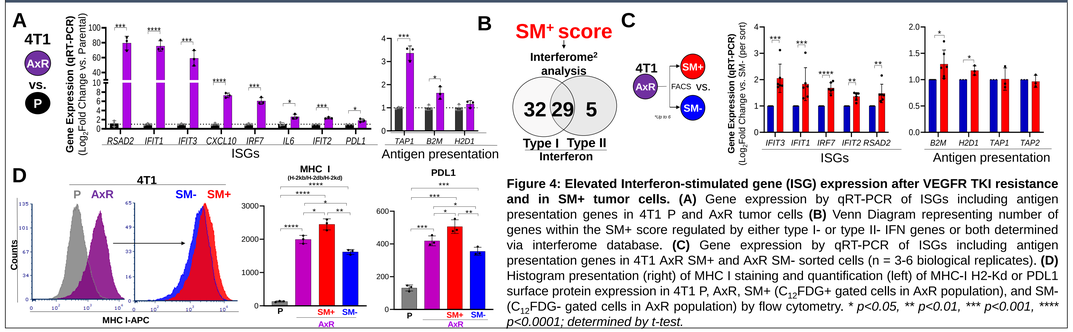

Figure 4: Elevated Interferon-stimulated gene (ISG) expression after VEGFR TKI resistance and in SM+ tumor cells. (A) Gene expression by qRT-PCR of ISGs including antigen presentation genes in 4T1 P and AxR tumor cells **(B)** Venn Diagram representing number of genes within the SM+ score regulated by either type I- or type II- IFN genes or both determined via interferome database. **(C)** Gene expression by qRT-PCR of ISGs including antigen presentation genes in 4T1 AxR SM+ and AxR SM- sorted cells (n = 3-6 biological replicates). **(D)** Histogram presentation (right) of MHC I staining and quantification (left) of MHC-I H2-Kd or PDL1 surface protein expression in 4T1 P, AxR, SM+ (C_{12}FDG+ gated cells in AxR population), and SM- (C_{12}FDG- gated cells in AxR population) by flow cytometry. * *p<0.05*, ** *p<0.01*, *** *p<0.001*, **** *p<0.0001; determined by t-test.*

⑤ SM+ cells promote activation of stimulated CD8 T-cells

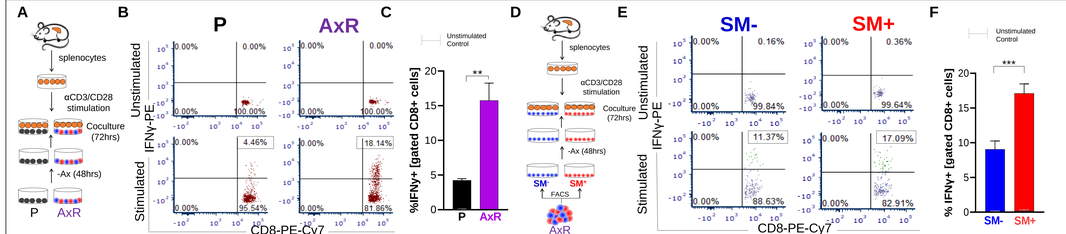

Figure 5: Differential activation of CD8 T-cells following coculture of stimulated splenocytes and tumor cell variants. (A) Schematic outline of tumor-splenocyte co-culture assay for 4T1 P and AxR model. **(B)** Dot plot representation and **(C)** quantification of %IFNγ+ gated CD8+ cells following coculture with unstimulated or stimulated splenocytes and 4T1 P or AxR tumor cells by flow cytometry. **(D)** Schematic outline of tumor-splenocyte coculture assay for live sorted AxR SM+ and SM- cells. **(E)** Dot plot representation and **(F)** quantification of %IFNγ+ gated CD8+ cells following coculture with unstimulated or stimulated splenocytes and AxR SM+ or SM- cells by flow cytometry. ** p<0.01; *** p<0.001.

⑥ SM+ tumors are more sensitive to adaptive immunity

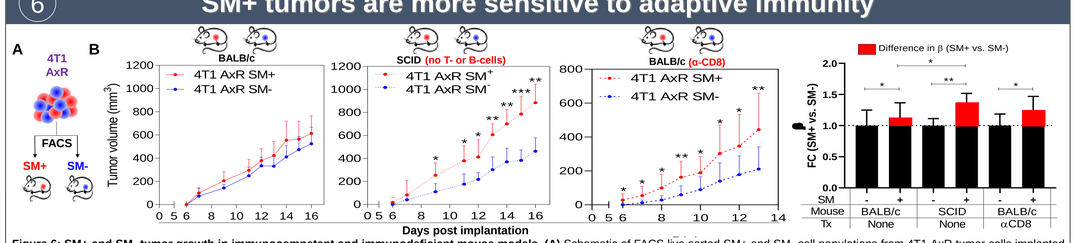

Figure 6: SM+ and SM- tumor growth in immunocompetent and immunodeficient mouse models. (A) Schematic of FACS live sorted SM+ and SM- cell populations from 4T1 AxR tumor cells implanted into mice for tumor growth evaluation. **(B)** Orthotopic tumor growth in Balb/c mice (n = 5;left), SCID mice (lacking T-and B-cells; n = 5;middle), and Balb/c mice treated with an anti-mouse CD8 antibody (pre-injection two days before implantation and continuously every 3 days; n = 10; right) to deplete CD8 T-cells. **(C)** Limited Gompertz modeling of tumor growth rate (β) of tumors in SM+ implanted mice compared to SM- implanted mice where red bars represent FC increased between SM+ vs. SM- groups (n = 34, Balb/c; n = 5, SCID, and n=10, Balb/c +αCD8). * *p<0.05*, ** *p<0.01*, *** *p<0.001; determined by t-test.*

⑦ SM+ tumors are more sensitive to PDL1 inhibition

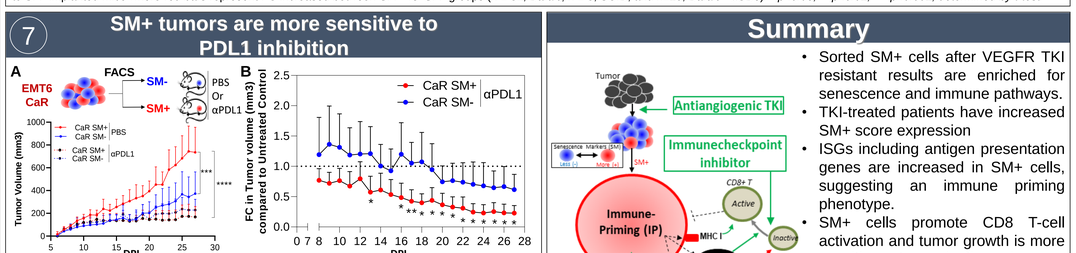

Figure 7: SM+ and SM- tumor growth following treatment with anti-PDL1. (A) Schematic of *in vivo* tumor growth of FACS sorted EMT6 CaR SM+ and SM- cells following treatment with PBS or anti-PDL1. **(B)** Orthotopic tumor growth and response to anti-PDL1 (n=5; Balb/c). **(C)** Comparison of EMT6 CaR SM+ and CaR SM- tumor response to anti-PDL1 treatment (FC compared to respective vehicle treated control) based on tumor volume. *** *p<0.001 and* ****p<0.0001 one-way ANOVA **(B)**. * p <0.05, ** p <0.01 determined by t-test comparing treatment groups **(C)**.

Summary

- Sorted SM+ cells after VEGFR TKI resistant results are enriched for senescence and immune pathways.
- TKI-treated patients have increased SM+ score expression
- ISGs including antigen presentation genes are increased in SM+ cells, suggesting an immune priming phenotype.
- SM+ cells promote CD8 T-cell activation and tumor growth is more sensitive to adaptive immune control.
- Blocking PDL1 had enhanced tumor growth inhibition of SM+ tumors.